Archives of Mechanics • Archiwum Mechaniki Stosowanej • 26, 6, pp. 981–994, Warszawa 1974

# Higher-order solutions for incompressible, three-dimensional boundary-layer flow at the stagnation point of a general body

H. D. PAPENFUSS (BOCHUM)

FIRST and second-order boundary-layer equations are derived for incompressible, three-dimensional flow near the stagnation point of a general convex body having two orthogonal symmetry planes. For this purpose, the "method of matched asymptotic expansions" is used. In the first-order equations, which are identical with the classical boundary-layer equations of Prandtl, the asymmetry at the stagnation point finds expression only through the parameter $c_1$, where $c_1$ is the ratio of the velocity gradients of the first-order potential flow at the stagnation point and varies between 0 (plane case) and 1 (axisymmetric case). In the second-order equations, which include the effects of body curvature and boundary-layer displacement, two further parameters enter into the problem: 1) the parameter $\varkappa$ ($0 \leqslant \varkappa \leqslant 1$) which is the ratio of the principal curvatures at the stagnation point; and 2) the parameter $c_2$ which is the ratio of the velocity gradients of the second-order potential flow at the stagnation point. Solutions of the second-order equations are given for a certain class of relations between these parameters and the parameter $c_1$ of the first-order theory.

Wyprowadzono równania pierwszego i drugiego rzędu warstwy przyściennej dla nieściśliwego trójwymiarowego przepływu w otoczeniu punktu stagnacji ogólnego ciała wypukłego, posiadającego dwie ortogonalne płaszczyzny symetrii. W tym celu wykorzystano "metodę dopasowanych rozwinięć asymptotycznych". W równaniach pierwszego rzędu, które są identyczne z klasycznymi równaniami warstwy przyściennej Prandtla, asymetria punktu stagnacji wyrażona jest tylko przez parametr $c_1$, oznaczający stosunek gradientów prędkości przepływu potencjalnego pierwszego rodzaju w punkcie stagnacji i zmieniający się od 0 (przypadek płaski) do 1 (przypadek osiowo symetryczny). W równaniach drugiego rzędu, w których uwzględnione zostały efekty krzywizny ciała i przemieszczenie warstwy przyściennej, występują dwa dalsze parametry: 1) parametr $\varkappa$ ($0 \leqslant \varkappa \leqslant 1$), będący stosunkiem głównych krzywizn w punkcie stagnacji, oraz 2) parametr $c_2$, oznaczający stosunek gradientów prędkości przepływu potencjalnego drugiego rzędu w punkcie stagnacji. Rozwiązania równań drugiego rzędu podano dla pewnej klasy zależności między tymi parametrami a parametrem pierwszego rodzaju $c_1$.

Выведены уравнения первого и второго порядка пограничного слоя для несжимаемого трехмерного течения в окрестности критической точки общего выпуклого тела, имеющего две ортогональные плоскости симметрии. С этой целью использован „метод сращиваемых асимптотических разложений" в уравнениях первого порядка, которые совпадают с классическими уравнениями пограничного слоя Прандтля, асимметрия критической точки выражена только через параметр $c_1$, обозначающий отношение градиентов скорости потенциального течения первого рода в критической точке и изменяющийся от нуля (плоский случай) до 1 (осесимметричный случай). В уравнениях второго порядка в которых учтены эффекты кривизны тела и перемещения пограничного слоя, выступают два дальнейших параметра: 1) параметр $\varkappa$ ($0 \leqslant \varkappa \leqslant 1$), будучий отношением главных кривизн в критической точке и 2) параметр $c_2$ обозначающий отношения градиентов скорости потенциального течения второго порядка в критической точке. Решения уравнений второго порядка даются для некоторого класса зависимостей между этими параметрами и параметром первого рода $c_1$.

## 1. Introduction

THE CALCULATION of the flow at a stagnation point is of practical importance since, for instance, the heat transfer attains a maximum at this point. In Fig. 1 are shown the streamline patterns for different types of stagnation point flow. We can distinguish between three basic types—viz. plane, axisymmetric, and general stagnation point flow.

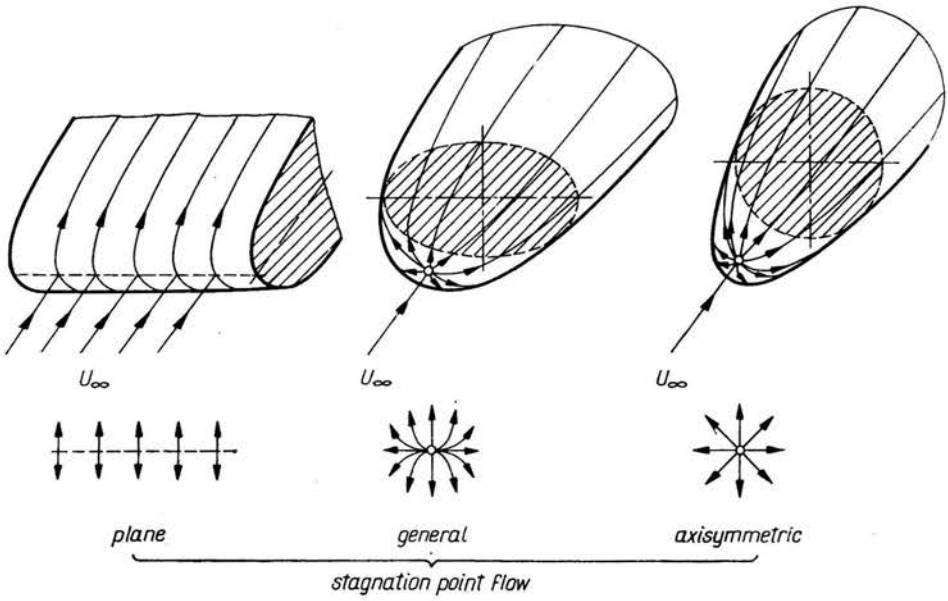


FIG. 1. Streamline patterns for different types of stagnation point flow.

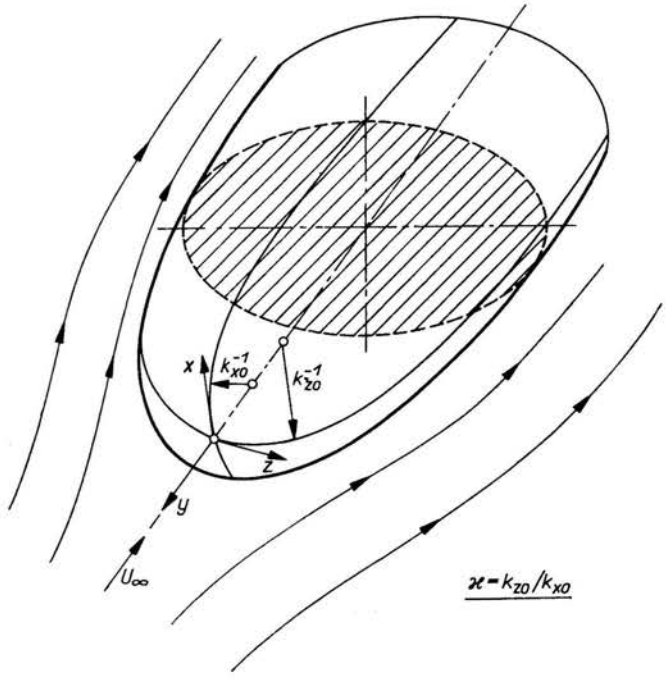


FIG. 2. Principal curvatures and the coordinate system at stagnation point.

The plane and axisymmetric cases have been investigated extensively by several authors for high Reynolds-number flow. We particularly draw attention to the work of M. VAN DYKE [1, 2], who went beyond the classical boundary-layer theory and thus included higher-order effects—viz. body curvature and boundary-layer displacement. It is common knowledge that these effects are not included in Prandtl's classical boundary-layer theory. Work at the second-order level is needed to gain a better insight into the effects of lower Reynolds-numbers as they are encountered in, for instance, high altitude flight and high Mach-number wind tunnel tests.

The object of this paper is to bridge the entire range of general incompressible stagnation point flows between the two extreme cases of plane and axisymmetric flows worked out by VAN DYKE.

The first-order boundary-layer equations for this problem were derived and solved by L. HOWARTH [3, 4]. Here, the second-order boundary-layer equations for this problem are derived and solved under the restriction that the body has two orthogonal symmetry planes and is placed in a stream parallel to its longitudinal axis (see Fig. 2). These equations are found from the full conservation laws by a perturbation analysis, using the "method of matched asymptotic expansions" with the inverse of the square root of a Reynolds-number as perturbation parameter.

## 2. General theory

### 2.1. Geometry and coordinate system

We consider a convex body having two orthogonal symmetry planes in a stream parallel to its longitudinal axis with free-stream velocity $U_\infty$. The properties of the fluid—density $\varrho$, viscosity $\mu$, specific heat $c$ and thermal conductivity $\lambda$—are constant.

If we slice the body at its planes of symmetry (Fig. 2), we obtain two intersection curves with different curvatures $k_{x0}$ and $k_{z0}$ at the stagnation point. The ratio of the two curvatures is denoted by $\varkappa$:

$$\varkappa = \frac{k_{z0}}{k_{x0}}, \tag{2.1}$$

where $k_{x0} \geqslant k_{z0}$. Therefore, $\varkappa = 0$ means that the body is plane at the stagnation point; $\varkappa = 1$ means that the body is axisymmetric at the stagnation point.

The coordinate system used here is orthogonal and follows the lines of principal curvature at the body. In the vicinity of the stagnation point, which is the origin of the coordinate system, the coordinate lines are identical with the intersection curves in Fig. 2. The third coordinate $y$ is measured along the normals erected on the body. In this coordinate system the line element has the following form:

$$(ds)^2 = [a_x(1+k_x y)dx]^2 + (dy)^2 + [a_z(1+k_z y)dz]^2, \tag{2.2}$$

where $a_x$ and $a_z$ are the Lamé-coefficients of the body surface ($y = 0$), $k_x$ and $k_z$ are the normal curvatures of the coordinate lines, measured in $x$ and $z$-direction, respectively. For simplicity we may, without loss of generality, suppose that $x$ and $z$ are so defined in magnitude that $a_x = a_z = 1$ at the stagnation point.

### 2.2. Basic equations

The flow and temperature field is determined by the conservation laws for mass, momentum, and energy:

$$\operatorname{div} \mathbf{w} = 0, \tag{2.3}$$

$$\varrho \left( \operatorname{grad} \frac{\mathbf{w}^2}{2} + (\operatorname{rot} \mathbf{w}) \times \mathbf{w} \right) = -\operatorname{grad} p - \mu \operatorname{rot}(\operatorname{rot} \mathbf{w}) , \tag{2.4}$$

$$\varrho c \mathbf{w} \operatorname{grad} T - \lambda \operatorname{div} \operatorname{grad} T = \mu \operatorname{Grad} \mathbf{w} \operatorname{def} \mathbf{w} + \mathbf{w} \operatorname{grad} p . \tag{2.5}$$

Herein $\mathbf{w}$ means the velocity vector, $p$ the pressure and $T$ the temperature. The boundary conditions are:

(2.6) 1) at the wall: $\mathbf{w} = 0, \quad T = T_w;$

(2.7) 2) at infinity: $|\mathbf{w}| = U_\infty, \quad p = p_\infty, \quad T = T_\infty.$

### 2.3. Outer expansions

For the outer expansions which are valid in a domain away from the surface, and for the inner expansions which are valid in a domain near to the surface, we use the well known perturbation parameter:

$$\varepsilon = \frac{1}{\sqrt{\mathrm{Re}}} , \tag{2.8}$$

with

$$\mathrm{Re} = \frac{U_\infty \varrho}{k_{x0} \mu} . \tag{2.9}$$

After VAN DYKE, the outer expansions for large Reynolds-numbers have the form:

$$\begin{aligned} \frac{u}{U_\infty} &= U_1 + \varepsilon U_2 + \ldots , \\ \frac{v}{U_\infty} &= V_1 + \varepsilon V_2 + \ldots , \\ \frac{w}{U_\infty} &= W_1 + \varepsilon W_2 + \ldots , \\ \frac{p - p_\infty}{\varrho \cdot U_\infty^2} &= P_1 + \varepsilon P_2 + \ldots , \\ \frac{T}{T_\infty} &= T_1 + \varepsilon T_2 + \ldots , \end{aligned} \tag{2.10}$$

where $u, v$, and $w$ are the velocity components in $x-$, $y-$, and $z$-direction, respectively. Substituting the expansions into the Eqs. (2.3)–(2.5) and collecting terms of the same order, we obtain the first-order equations for the unknowns $U_1$, $V_1$, $W_1$, $P_1$, and $T_1$ and the second-order equations for the unknowns $U_2$, $V_2$, $W_2$, $P_2$, and $T_2$. These equations can be found, for instance, in VAN DYKE's paper [1]. The solutions of these equations have the following properties:

1) first and second-order velocities can be calculated from the irrotational condition (potential flow);

2) first and second-order pressures can be calculated from first and second-order Bernoulli's equation:

$$P_1+\frac{1}{2}(U_1^2+V_1^2+W_1^2)=\frac{1}{2}, \tag{2.11}$$

$$P_2+U_1U_2+V_1V_2+W_1W_2=0; \tag{2.12}$$

3) first and second-order temperatures are

$$T_1=1, \tag{2.13}$$

$$T_2=0. \tag{2.14}$$

The boundary conditions at the wall for the outer expansions are obtained by matching with the inner expansions.

For the inner equations we shall need the surface values of the outer velocities. For small distances from the stagnation point we expand these quantities in Taylor-series. Using the irrotational condition, we obtain:

$$\frac{u(x,0,z)}{U_\infty}=k_{x0}\,x\,(U_{11}+\varepsilon U_{21}+\ldots), \tag{2.15}$$

$$\begin{aligned}\frac{w(x,0,z)}{U_\infty}&=k_{x0}\,z(W_{11}+\varepsilon W_{21}+\ldots)\\&=k_{x0}z(c_1U_{11}+\varepsilon c_2U_{21}+\ldots).\end{aligned} \tag{2.16}$$

The following abbreviations are used:

$$c_1\equiv\frac{(\partial W_1/\partial z)_0}{(\partial U_1/\partial x)_0}=\frac{W_{11}}{U_{11}}, \tag{2.17}$$

$$c_2\equiv\frac{(\partial W_2/\partial z)_0}{(\partial U_2/\partial x)_0}=\frac{W_{21}}{U_{21}}. \tag{2.18}$$

The parameter $c_1$ is the ratio of the velocity gradients of the first-order outer flow at the stagnation point in the two orthogonal directions. Hence, $c_1$ characterizes the asymmetry in the first-order outer flow at the stagnation point. A stagnation point flow is defined to be plane if $c_1=0$; a stagnation point flow is defined to be axisymmetric if $c_1=1$.

The parameter $c_2$ is the ratio of the velocity gradients of the second-order outer flow at the stagnation point in the two orthogonal directions. Hence, $c_2$ characterizes the asymmetry in the second-order outer flow at the stagnation point. The parameter $c_2$ can attain any value, depending on geometry and flow conditions.

The quantities $U_{21}$ and $W_{21}$ (and hence $c_2$) depend on the growth of the first-order inner solution and are obtained by solving the elliptical differential equation for the second-order outer flow. For the time being, it is not possible to calculate $U_{21}$ and $W_{21}$ when the first-order inner solution leads to separation. We therefore restrict ourselves to body configurations free of separation.

**2.4. Inner expansions**

The inner expansions are written in the inner variable:

$$\eta = k_{x0}\, y \sqrt{U_{11}\,\mathrm{Re}} \tag{2.19}$$

The following expressions are so given that the continuity equation is automatically satisfied. The leading term in the expansions corresponds to Prandtl's classical boundary-layer theory. The second terms represent the influence of boundary-layer displacement (index 2d) and body curvature (index 2c). It is possible to split up the second-order contributions, since the second-order boundary-layer equations are—as we shall see—linear differential equations.

The inner expansions have the following form:

$$\frac{u}{U_\infty} = U_{11} k_{x0} x \left\{ f_1'(\eta) + \varepsilon \frac{U_{21}}{U_{11}} f_{2d}'(\eta) + \frac{\varepsilon}{\sqrt{U_{11}}} [f_{2c}'(\eta) - \varkappa \eta f_1'(\eta)] \right\} + \ldots \tag{2.20}$$

$$\frac{v}{U_\infty} = -\varepsilon \sqrt{U_{11}} \left\{ [f_1(\eta) + c_1 g_1(\eta)] + \varepsilon \frac{U_{21}}{U_{11}} [f_{2d}(\eta) + c_1 g_2(\eta)] + \right. \tag{2.21}$$

$$\left. + \frac{\varepsilon}{\sqrt{U_{11}}} [f_{2c}(\eta) + c_1 g_{2c}(\eta) - (1+\varkappa)\eta (f_1(\eta) + c_1 g_1(\eta))] \right\} + \ldots$$

$$\frac{w}{U_\infty} = c_1 U_{11} k_{x0} z \left\{ g_1'(\eta) + \varepsilon \frac{U_{21}}{U_{11}} g_{2d}'(\eta) + \frac{\varepsilon}{\sqrt{U_{11}}} [g_{2c}'(\eta) - \eta g_1'(\eta)] \right\} + \ldots \tag{2.22}$$

$$\frac{p - p_\infty}{\varrho U_\infty^2} = \frac{1}{2} - \frac{1}{2} U_{11}^2 k_{x0}^2 x^2 \left\{ \bar{p}_1(\eta) + \varepsilon \frac{U_{21}}{U_{11}} \bar{p}_{2d}(\eta) + \frac{\varepsilon}{\sqrt{U_{11}}} \bar{p}_{2c}(\eta) + \ldots \right\} \tag{2.23}$$

$$- \frac{1}{2} c_1^2 U_{11}^2 k_{x0}^2 z^2 \left\{ \tilde{p}_1(\eta) + \varepsilon \frac{U_{21}}{U_{11}} \tilde{p}_{2d}(\eta) + \frac{\varepsilon}{\sqrt{U_{11}}} \tilde{p}_{2c}(\eta) + \ldots \right\}$$

$$\frac{T - T_{w0}}{T_\infty - T_{w0}} = \vartheta_1(\eta) + \varepsilon \frac{U_{21}}{U_{11}} \vartheta_{2d}(\eta) + \frac{\varepsilon}{\sqrt{U_{11}}} \vartheta_{2c}(\eta) + \ldots \tag{2.24}$$

Dashes indicate differentiation with respect to $\eta$. The index wo refers to the stagnation point. Further, we need expansions of the geometrical quantities in the vicinity of the stagnation point:

$$a_x = 1 + \ldots \tag{2.25}$$

$$a_z = 1 + \ldots \tag{2.26}$$

$$k_x = k_{x0} + \ldots \tag{2.27}$$

$$k_z = \varkappa k_{x0} + \ldots \tag{2.28}$$

These expressions can be substituted into the full conservation laws. Then, terms of the same order are again to be collected. Terms of order 0(1) yield the first-order inner

equations, terms of order $0(\varepsilon)$ yield the second-order inner equations. In cases in which the equations are linear, the following linear operators are used:

$$\mathscr{L}_1(F) = F''+\mathrm{Pr}(f_1+c_1g_1)F', \tag{2.29}$$

$$\mathscr{L}_2(F;G) = F'''+(f_1+c_1g_1)F''-2f_1'F'+(F+c_1G)f_1'', \tag{2.30}$$

$$\mathscr{L}_3(F;G) = F'''+(f_1+c_1g_1)F''-2c_1g_1'F'+(G+c_1F)g_1'', \tag{2.31}$$

$F$ and $G$ are functions of $\eta$. The Prandtl-number is defined as

$$\mathrm{Pr} = \frac{\mu c}{\lambda}. \tag{2.32}$$

The *first-order inner equations* are:

$$f_1'''+(f_1+c_1g_1)f_1''-f_1'^2 = -\bar{p}_1, \tag{2.33}$$

$$g_1'''+(f_1+c_1g_1)g_1''-c_1g_1'^2 = -c_1\tilde{p}_1, \tag{2.34}$$

$$\bar{p}_1' = 0, \tag{2.35}$$

$$\tilde{p}_1' = 0, \tag{2.36}$$

$$\mathscr{L}_1(\vartheta_1) = 0. \tag{2.37}$$

The boundary conditions for the foregoing equations are:

$$\eta = 0: \quad f_1 = f_1' = g_1 = g_1' = \vartheta_1 = 0, \tag{2.38}$$

$$\eta \to \infty: \quad f_1' = g_1' = \bar{p}_1 = \tilde{p}_1 = \vartheta_1 = 1. \tag{2.39}$$

For the pressures we obtain at once the following analytic solution:

$$\bar{p}_1 = \tilde{p}_1 = 1. \tag{2.40}$$

We find that in the first-order equations, derived from Prandtl's classical boundary-layer theory, the geometric asymmetry at the stagnation point, expressed by $\varkappa$, does not appear explicitly. The asymmetric nature of the flow at a general stagnation point finds expression only through the parameter $c_1$, which reflects the asymmetry in the first-order outer flow.

For the displacement effect, we obtain the following *second-order inner equations*:

$$\mathscr{L}_2(f_{2d}; g_{2d}) = -\bar{p}_{2d}, \tag{2.41}$$

$$\mathscr{L}_3(g_{2d}; f_{2d}) = -c_1\tilde{p}_{2d}, \tag{2.42}$$

$$\bar{p}_{2d}' = 0, \tag{2.43}$$

$$\tilde{p}_{2d}' = 0, \tag{2.44}$$

$$\mathscr{L}_1(\vartheta_{2d}) = -\mathrm{Pr}(f_{2d}+c_1g_{2d})\vartheta_1'. \tag{2.45}$$

The boundary conditions are:

$$\eta = 0: \quad f_{2d} = f_{2d}' = g_{2d} = g_{2d}' = \vartheta_{2d} = 0, \tag{2.46}$$

$$\left.\begin{aligned} &\eta \to \infty: f_{2d}' = 1, \quad g_{2d}' = \frac{c_2}{c_1}, \\ &\bar{p}_{2d} = 2, \quad \tilde{p}_{2d} = 2\cdot\frac{c_2}{c_1}, \\ &\vartheta_{2d} = 0. \end{aligned}\right\} \tag{2.47}$$

For the pressures, we obtain at once the analytic solutions:

$$\bar{p}_{2a} = 2, \tag{2.48}$$

$$\tilde{p}_{2a} = 2 \cdot \frac{c_2}{c_1}. \tag{2.49}$$

In the particular case $c_1 = c_2$, the solutions of the Eqs. (2.41)–(2.45) are

$$f_{2a} = \frac{1}{2}(f_1 + \eta f_1'), \tag{2.50}$$

$$g_{2a} = \frac{1}{2}(g_1 + \eta g_1'), \tag{2.51}$$

$$\vartheta_{2a} = \frac{1}{2}\eta\vartheta_1'. \tag{2.52}$$

For the curvature effect, we obtain the following *second-order inner equations*:

$$\begin{aligned}\mathscr{L}_2(f_{2c}, g_{2c}) = {} & -\bar{p}_{2c} + (1+\varkappa)\eta[(f_1 + c_1 g_1)f_1'' - f_1'^2] \\ & -(1-\varkappa)[f_1'' + (f_1 + c_1 g_1)f_1' - \eta],\end{aligned} \tag{2.53}$$

$$\begin{aligned}\mathscr{L}_3(g_{2c}, f_{2c}) = {} & -c_1\tilde{p}_{2c} + (1+\varkappa)\eta[(f_1 + c_1 g_1)g_1'' - c_1 g_1'^2] \\ & +(1-\varkappa)[g_1'' + (f_1 + c_1 g_1)g_1' - c_1\eta],\end{aligned} \tag{2.54}$$

$$\bar{p}_{2c}' = -2f_1'^2, \tag{2.55}$$

$$\tilde{p}_{2c}' = -2\varkappa g_1'^2, \tag{2.56}$$

$$\mathscr{L}_1(\vartheta_{2c}) = \{(1+\varkappa)(\mathrm{Pr}\eta(f_1 + c_1 g_1) - 1) - \mathrm{Pr}(f_{2c} + c_1 g_{2c})\}\vartheta_1'. \tag{2.57}$$

The boundary conditions are:

$$\eta = 0: \quad f_{2c} = f_{2c}' = g_{2c} = g_{2c}' = \vartheta_{2c} = 0, \tag{2.58}$$

$$\left.\begin{aligned}\eta \to \infty: \quad & f_{2c}'' = -(1-\varkappa), \quad g_{2c}'' = 1-\varkappa, \\ & \bar{p}_{2c}' = -2, \quad \tilde{p}_{2c}' = -2\varkappa, \\ & \vartheta_{2c} = 0.\end{aligned}\right\} \tag{2.59}$$

For the pressures, we obtain the analytic solutions:

$$\bar{p}_{2c} = -f_1'' - (f_1 + c_1 g_1)f_1' - \eta(1-c_1) - (1+c_1)\beta_1 + c_1\gamma_1 - c_1\int_0^\eta (1 - f_1' g_1')\,d\eta, \tag{2.60}$$

$$\tilde{p}_{2c} = \frac{\varkappa}{c_1}\left(-g_1'' - (f_1 + c_1 g_1)g_1' + \eta(1-c_1) - (1+c_1)\beta_1 + \gamma_1 - \int_0^\eta (1 - f_1' g_1')\,d\eta\right). \tag{2.61}$$

We have used the abbreviations

$$\beta_1 \equiv \int_0^\infty \left(1 - \frac{f_1' + c_1 g_1'}{1+c_1}\right) d\eta = \frac{1}{1+c_1} \lim_{\eta\to\infty}\left((\eta - f_1) + c_1(\eta - g_1)\right) \tag{2.62}$$

and

$$\gamma_1 \equiv \int_0^\infty (1-f_1' g_1')\,d\eta. \tag{2.63}$$

The boundary conditions at $\eta \to \infty$ for the first and second-order equations are supplied by matching the inner and outer expansions. The procedure of matching can be found in, for instance, Van Dyke's paper [1].

### 2.5. Boundary-layer characteristics

As a consequence of the decrease in velocity in the boundary layer, the external flow is displaced outwards. For plane and axisymmetric flow, the definition of a displacement surface is well known. After F. K. MOORE [5] and R. SEDNEY [6], it is possible to define such a fictitious surface even for three-dimensional flow. The local distance between the wall and the displacement surface — i.e., the displacement thickness—is such defined that the mass-flow defect due to the effect of friction is compensated.

We write the displacement thickness $D^*$ at the stagnation point as asymptotic expansion in terms of the perturbation parameter $\varepsilon$:

$$D^* = \frac{\varepsilon}{k_{x0}\sqrt{U_{11}}}\left\{\delta_1^* + \varepsilon\left(\frac{U_{21}}{U_{11}}\delta_{2a}^* + \frac{1}{\sqrt{U_{11}}}\delta_{2c}^*\right)\right\} + \ldots \tag{2.64}$$

We obtain:

$$\delta_1^* = \frac{1}{1+c_1}\lim_{\eta\to\infty}\left((\eta - f_1) + c_1(\eta - g_1)\right) = \beta_1, \tag{2.65}$$

$$\delta_{2a}^* = \frac{1}{1+c_1}\left\{\lim_{\eta\to\infty}\left[(\eta - f_{2a}) + c_1\left(\frac{c_2}{c_1}\eta - g_{2a}\right)\right] - (1+c_2)\,\delta_1^*\right\}, \tag{2.66}$$

$$\delta_{2c}^* = \frac{1}{1+c_1}\left\{\lim_{\eta\to\infty}\left[\left(-f_{2c} - \frac{1}{2}(1-\varkappa)\eta^2\right) + c_1\left(-g_{2c} + \frac{1}{2}(1-\varkappa)\eta^2\right)\right] + \frac{1}{2}(1-\varkappa)(1-c_1)\,\delta_1^{*2}\right\}. \tag{2.67}$$

The Eq. (2.65) has already been given by P.A. LIBBY [7].

The components of the wall shear stress vector, expressed by the dimensionless coefficients $c_{fx}$ and $c_{fz}$, and the wall heat transfer, expressed by the Stanton-number, can be written in the following form:

$$c_{fx} = \frac{\tau_{xy}}{\varrho U_\infty^2} = \varepsilon U_{11}^{\frac{3}{2}} k_{x0} x\left\{f_1''(0) + \varepsilon\left[\frac{U_{21}}{U_{11}} f_{2a}''(0) + \frac{1}{\sqrt{U_{11}}} f_{2c}''(0)\right]\right\} + \ldots, \tag{2.68}$$

$$c_{fz} = \frac{\tau_{zy}}{\varrho U_\infty^2} = \varepsilon c_1 U_{11}^{\frac{3}{2}} k_{x0} z\left\{g_1''(0) + \varepsilon\left[\frac{U_{21}}{U_{11}} g_{2a}''(0) + \frac{1}{\sqrt{U_{11}}} g_{2c}''(0)\right]\right\} + \ldots, \tag{2.69}$$

$$\mathrm{St} = \frac{q_{w0}}{\varrho c U_\infty (T_{w0} - T_\infty)} = -\varepsilon\frac{\sqrt{U_{11}}}{\mathrm{Pr}}\left\{\vartheta_1'(0) + \varepsilon\left[\frac{U_{21}}{U_{11}}\vartheta_{2a}'(0) + \frac{1}{\sqrt{U_{11}}}\vartheta_{2c}'(0)\right]\right\} \ldots \tag{2.70}$$

### 3. Results and discussion

The first and second-order boundary-layer equations presented for incompressible, three-dimensional stagnation point flow have been integrated numerically using the method of Runge-Kutta. The parameter $c_1$, which reflects the asymmetry of the first-order outer flow at the stagnation point, was varied between 0 (plane case) and 1 (axisymmetric case). Figures 3–5 show the results of the first-order theory. All these results are from Prandtl's theory: displacement thickness, wall shear stresses, and wall heat transfer. We note that the variation of $c_1$ has little influence on the $x$-component of the shear stress if

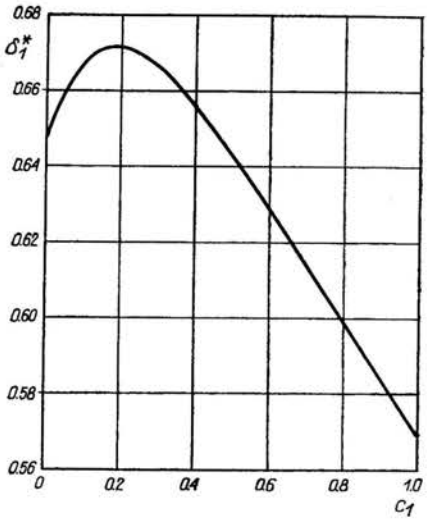


FIG. 3. First-order displacement thickness.

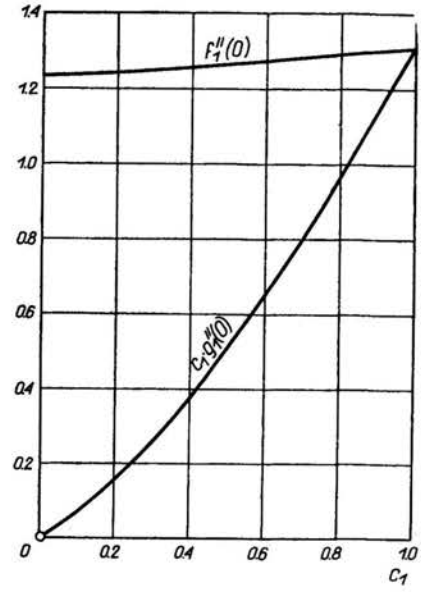


FIG. 4. First-order wall shear stresses.

we assume that the quantity $U_{11}$ in the Eq. (2.68) is constant ($U_{11} = 1$ for parabola and axisymmetric paraboloid). Further, we see that the first-order heat transfer increases almost linearly with $c_1$. If we compare two parabolic bodies, plane and axisymmetric, with the same nose radius in a stream under identical conditions, we find that the heat transfer at the stagnation point of the axisymmetric body lies about 30 per cent higher than the heat transfer at the plane body.

In Figs. 6–8, the effect due to boundary-layer displacement is shown. In addition to the parameter $c_1$, we now have in the displacement problem the parameter $c_2$, which reflects the asymmetry of the second-order outer flow at the stagnation point. For the two extreme cases of plane and axisymmetric flow, we obtain $c_2 = c_1$. We restricted ourselves to configurations where always $c_2 = c_1$.

Furthermore, we have to reflect upon the quantity $U_{21}$, which is the velocity gradient of the second-order outer flow in the $x$-direction, and which appears in the equations for the boundary-layer characteristics. Calculating $U_{21}$ is extremely difficult, since an elliptical differential equation has to be solved. For the cases we known — the plane and axisymmetric

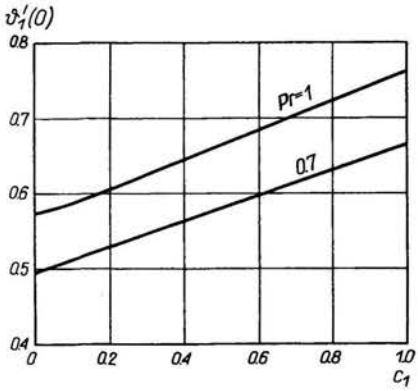


FIG. 5. First-order wall heat transfer.

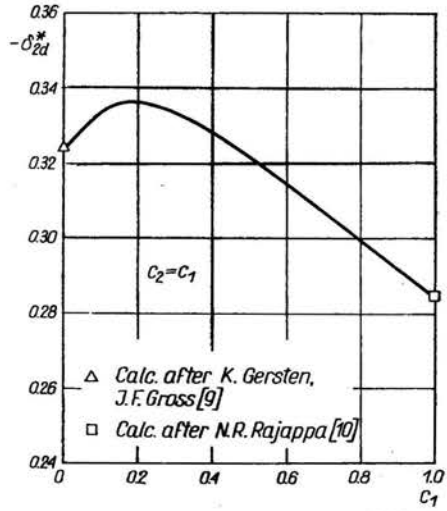


FIG. 6. Second-order displacement thickness due to displacement.

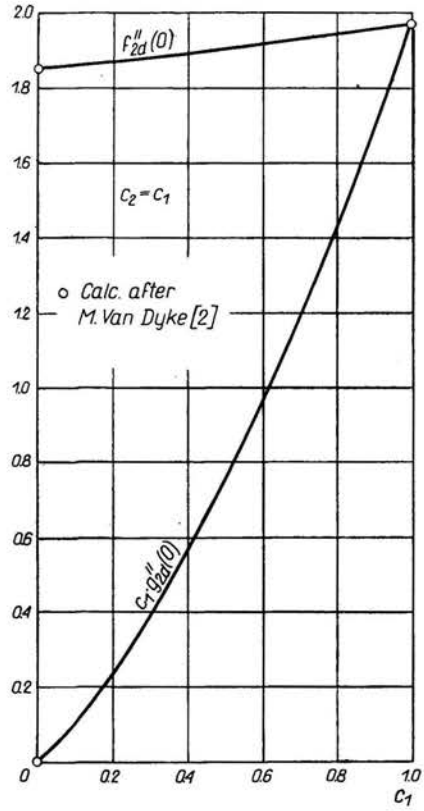


FIG. 7. Second-order wall shear stresses due to displacement.

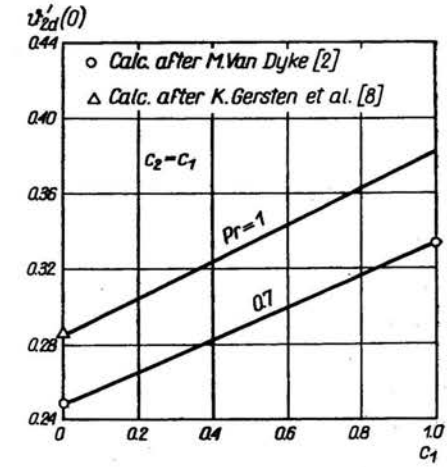


FIG. 8. Second-order wall heat transfer due to displacement.

semi-infinite body — $U_{21}$ turns out to be negative. So far we do not have sufficiently general information about the behaviour of this quantity $U_{21}$. We may therefore presume for the time being that $U_{21}$ is also negative in the general case.

We note from the figures that the second-order quantities, corresponding to the wall shear stresses and the wall heat transfer, are positive for all values of $c_1$. Since these quantities have to be multiplied by the presumably negative quantity $U_{21}$, we may conclude that the shear stresses and the heat transfer at a general stagnation point are in

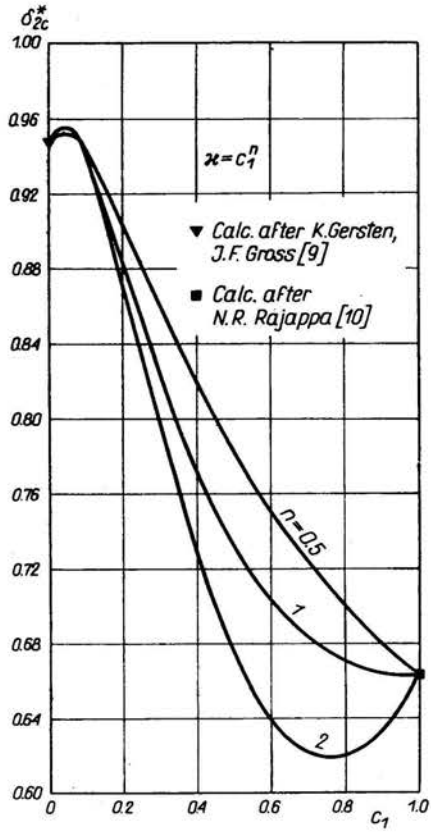


FIG. 9. Second-order displacement thickness due to body curvature.

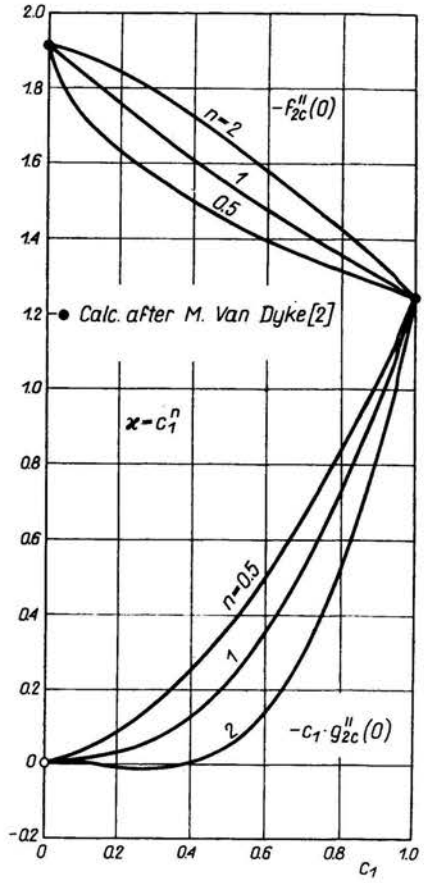


FIG. 10. Second-order wall shear stresses due to body curvature.

principle reduced due to boundary-layer displacement. The displacement thickness, on the contrary, shows the opposite behaviour.

In Figs. 9–12 is shown the effect due to body curvature. In addition to the parameter $c_1$, we now have in the curvature problem the parameter $\varkappa$, which reflects the geometric asymmetry at the stagnation point, as against the parameter $c_2$ which enters the displacement problem. We have restricted ourselves to body configurations characterized by the coupling

$$\varkappa = c_1^n,$$

and studied the cases $n = 0.5; 1; 2$. For instance, in the case of an elliptical paraboloid we have $n = 1$.

For $c_1 = 0$—that is the plane case—only the effect due to longitudinal curvature is present. From the signs of the second-order quantities, we find that in this case the displacement thickness is increased, but the shear stresses and the heat transfer at the stagnation point are reduced due to surface curvature. For $c_1 = 1$—that is, the axisymmetric case—the effects of both the longitudinal and transverse curvature are present.

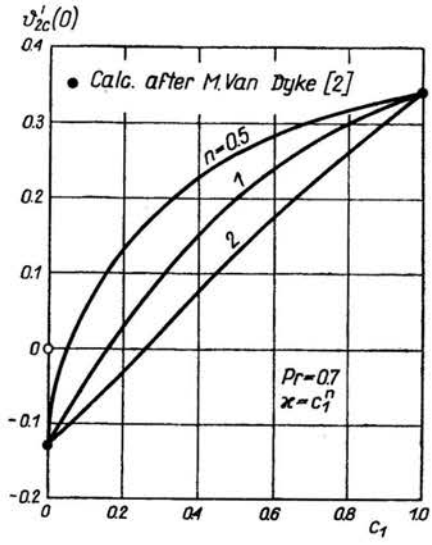


FIG. 11. Second-order wall heat transfer due to body curvature.

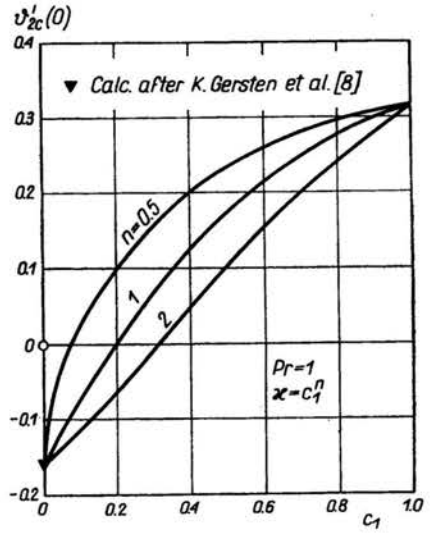


FIG. 12. Second-order wall heat transfer due to body curvature.

From the signs, we find that in this case the displacement thickness and the heat transfer are increased, whereas the shear stress is reduced as against classical boundary-layer theory.

There is a change in sign for the second-order heat transfer due to surface curvature, where the effects of longitudinal and transverse curvature cancel each other. For sufficiently large values of $c_1$, the effect of transverse curvature predominates.

Summarizing we can say: As against classical boundary-layer theory, the curvature effect can either reduce or augment the shear stresses and the heat transfer at a stagnation point, depending on the geometry, whereas the displacement effect always reduces these quantities. The difficulty that remains is to calculate the second-order outer flow, and hence $U_{21}$ and $W_{21}$, for a given set of flow conditions.

## References

1. M. VAN DYKE, *Higher approximations in boundary-layer theory.* Part 1. *General analysis*, J. Fluid Mech., **14**, 161–177, 1962.
2. M. VAN DYKE, *Higher approximations in boundary-layer theory.* Part 2. *Application to leading edges*, J. Fluid Mech., **14**, 481–495. 1962.

3. L. HOWARTH, *The boundary-layer in three-dimensional flow.* Part I. *Derivation of the equations for flow along a general curved surface*, Phil. Magazine, **42**, 239–243, 1951.
4. L. HOWARTH, *The boundary layer in three-dimensional flow.* Part II. *The flow near a stagnation point*, Phil. Magazine, **42**, 1433–1440, 1951.
5. F. K. MOORE, *Displacement effect of a three-dimensional boundary-layer*, NACA-Rep., 1124, 1953.
6. R. SEDNEY, *Some aspects of three-dimensional boundary-layer flows*, Quart. Appl. Math., **15**, 2, 113–122, 1957.
7. P. A. LIBBY, *Heat and mass transfer at a general three-dimensional stagnation point*, AIAA Journal, **5**, 3, 507–517, 1967.
8. K. GERSTEN, J. F. GROSS, G. G. BÖRGER, *Die Grenzschicht höherer Ordnung an der Staulinie eines schiebenden Zylinders mit starkem Absaugen oder Ausblasen*, Zeitschr. Flugwiss., **20**, 330–341, 1972.
9. K. GERSTEN, J. F. GROSS, *Mass-transfer effects on higher-order boundary-layer solutions: The leading edge of a swept cylinder*, Int. J. Heat Mass Transfer, **16**, 65–79, 1973.
10. N. R. RAJAPPA, *Die inkompressible Grenzschicht höherer Ordnung am rotationssymmetrischen Staupunkt bei starkem Absaugen oder Ausblasen*, Zeitschr. angewandte Math.- Physik, ZAMP, **24**, 317–329, 1973.

INSTITUTE FOR THERMO- AND FLUIDDYNAMICS
UNIVERSITY OF BOCHUM, WEST-GERMANY.

*Received October* 15, 1973.